Research Article

Transformation of Thermal Expansion from Large Volume Contraction to Nonlinear Strong Negative Thermal Expansion in PbTiO₃−Bi(Co₁₋ₓFeₓ)O₃ Perovskites

Zhao Pan,*,[#] Xingxing Jiang,[#] Runze Yu, Yang Ren, Zheshuai Lin, Jun Chen,* Masaki Azuma, and Xianran Xing

Cite This: *ACS Appl. Mater. Interfaces* 2022, 14, 23610−23616
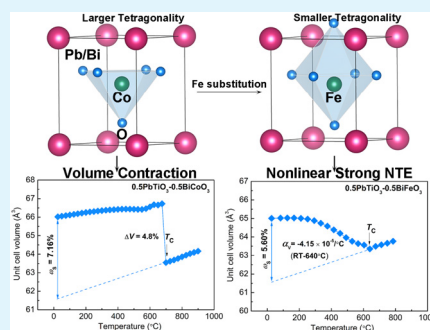
Read Online

ACCESS | 📊 Metrics & More | 📖 Article Recommendations | 🆘 Supporting Information

ABSTRACT: Controlling negative thermal expansion (NTE) is an important topic in the study of NTE materials. Generally, a large magnitude of NTE with a wide NTE operation temperature window is preferable for applications of NTE materials, as a stronger NTE can be used to tailor the coefficient of thermal expansion (CTE) of materials with positive thermal expansion by forming composites more efficiently. However, controlling the NTE in single-phase materials is still a significant challenge. In present study, we proposed a promising method to control the thermal expansion from large volume contraction in a limited temperature widow ($x = 0$, $\Delta V = -4.8\%$, 675−700 °C) to a nonlinear strong NTE over a wider temperature range ($x = 0.8$, $\bar{\alpha}_V = -6.12 \times 10^{-5}/°C$, RT to 600 °C) by means of adjusting the proportion of cations with different ferroelectric activities in $0.5PbTiO_3-0.5Bi(Co_{1-x}Fe_x)O_3$ ferroelectrics. The obtained NTE was stronger than many of the currently available NTE materials, and the operation window of NTE was also in an extended temperature range. The unusual transformation is well explained by the spontaneous volume ferroelectrostriction effect, which was evidenced by joint experimental and theoretical studies. The present work not only may pave the way for controllable large NTE in PbTiO₃-based ferroelectrics but also could be extended to magnetic NTE materials, whose NTE is coupled with magnetism.

KEYWORDS: *negative thermal expansion, perovskite, tetragonality, synchrotron X-ray diffraction, phase transition*
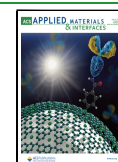
INTRODUCTION

Thermal expansion is a long-standing issue in areas such as machinery, electronics, optics, and aerospace engineering.[1−4] A mismatch in thermal expansion can induce many serious problems, including functional deterioration, failure, or even cracking in devices.[3] The discovery of negative thermal expansion (NTE) materials, whereby the volume contracts instead of expanding upon heating, has potential engineering applications in thermal expansion control. Materials with a controllable coefficient of thermal expansion (CTE) can be achieved by forming composites between NTE materials and normal positive thermal expansion materials. For example, near zero thermal expansion (ZTE) can be realized in composites consisting of NTE materials and general thermal expansion materials, such as ZrW_2O_8/ZrO_2 composites,[5] $Mn_3Cu_{0.5}A_{0.5}N$ (A = Ni, Sn)/Cu composites,[6] and $0.5PbTiO_3-0.5(Bi_{0.9}La_{0.1})FeO_3$/Cu core−shell composites.[7] Nevertheless, disadvantages such as thermal stress at the interface can occur in these composites, hindering the potential applications of NTE materials. Once controllable CTE can be realized in individual single-phase materials, we can expect to overcome these drawbacks and ensure the effective and favorable use of NTE materials.

Controllable NTE is interesting from the fundamental viewpoint of understanding the nature of thermal expansion and practical thermal-expansion-control engineering, especially for individual single-phase NTE materials.[8,9] Over the past few decades, we have witnessed many types of chemical modifications of various NTE materials.[3,10−18] In NTE control for the well-known ZrW_2O_8-based framework NTE materials, single-phase NTE showed little dependence on the material composition, and CTE varied only within a very limited range ($\bar{\alpha}_V = (-2.2$ to $-2.6) \times 10^{-5}/°C$) by chemical modifications. These characteristics were mainly attributed to the low solid solubility limit.[10] However, the $Al_{2x}(Hf,Mg)_{1-x}(WO_4)_3$ single-phase ceramics had a relatively wide CTE range of (-0.23 to $0.45) \times 10^{-5}/°C$,[14] crossing from negative to positive thermal expansion through chemical modification, and favorable ZTE was achieved. More recently, large isotropic NTE was observed

in SmS,[13] suggesting a correlation with the valence fluctuation of Sm. Many substitutions have been attempted to modify the CTE of SmS.[13,19] A near ZTE has also been established for $Sm_{0.80}La_{0.20}S$ in a temperature range of 100−500 K.[13] Therefore, studying the complex interplay between phonons, electrons, and lattices can help us to control NTE more efficiently, especially for large NTE over a wide temperature range. Materials with controllable NTE in a wide temperature range would also be favorable in practical applications of NTE materials. However, achieving controllable NTE in individual single-phase NTE materials remains a great challenge.

Among the available NTE materials, $PbTiO_3$ (PT)-based perovskite-type (ABO_3) ferroelectrics have generally exhibited unusual NTE during the ferroelectric-to-paraelectric (FE-to-PE) phase transition.[20] $PbTiO_3$ is a typical tetragonal perovskite ferroelectric compound with $c/a = 1.064$, which also exhibits NTE in a wide temperature range from room temperature up to its Curie temperature ($T_C = 490$ °C).[21] Because shrinkage of unit cell volume in PT-based ferroelectrics will mainly occur in the c-axis of their tetragonal phase, the c/a can be used to trace NTE.[22,23] Indeed, a large NTE over a wide temperature range was successfully achieved in PT-based ferroelectrics with enhanced c/a, such as $Pb_{0.94}Cd_{0.06}TiO_3$ ($c/a = 1.069$, $\bar{\alpha}_V = -2.40 \times 10^{-5}$ °C^{-1}, RT to 500 °C) and $0.4PbTiO_3-0.6BiFeO_3$ ($c/a = 1.165$, $\bar{\alpha}_V = -3.92 \times 10^{-5}$ °C^{-1}, RT to 650 °C).[24,25] More recently, colossal volume contraction as large as −4.8% accompanied by the FE-to-PE phase transition was observed in a $0.5PbTiO_3-0.5BiCoO_3$ compound with a large c/a value of 1.17,[26] which had never been observed in PT-based ferroelectric compounds. However, large volume shrinkage could only be observed in a relatively narrow temperature window limiting its use for practical applications. Because of the flexible structure of PT, the CTE can be easily tailored through general chemical substitutions by the A-site Pb or B-site Ti cations, or A/B-site cosubstitutions.[3] Additionally, temperature-dependent spontaneous polarization (P_S) and lattice dynamics from Raman analysis suggested that ferroelectric behavior was closely related to the NTE property of PT-based compounds.[27,28] In terms of NTE materials applications, a key point is to realize a large magnitude of NTE within a wide temperature window. Herein, we demonstrated an effective method for tailoring the giant but narrow temperature range of NTE in $0.5PbTiO_3-0.5BiCoO_3$ by modifying the ratio of cations with different ferroelectric activities. In this work, ferroelectric activity can be indicated by the P_S displacement in the oxygen polyhedron.[29,30] The investigated system was $0.5PbTiO_3-0.5BiCo_{1-x}Fe_xO_3$ ($0 \leq x \leq 1$), in which Fe with moderately ferroelectric active (0.45 Å) was used to replace that of Co^{3+} with strongly ferroelectric active (0.69 Å) in $0.5PbTiO_3-0.5BiCoO_3$. The volume contraction of $0.5PbTiO_3-0.5BiCo_{1-x}Fe_xO_3$ gradually decreases with Fe substitution and finally transformed from large volume contraction in a narrow temperature range to nonlinear strong NTE over a wide temperature range. The detailed crystal structure, thermal expansion, and related P_S displacements were systematically studied by experimental and first-principles calculations.

■ EXPERIMENTAL SECTION

A series of $0.5PbTiO_3-0.5BiCo_{1-x}Fe_xO_3$ ($0 \leq x \leq 1$) compounds were prepared by the high-pressure and high-temperature (HP-HT) method. The raw materials of PbO, TiO_2, Bi_2O_3, Co_3O_4, and Fe_2O_3 were thoroughly mixed according to the stoichiometric ratio. Details

regarding the HP-HT synthesis were provided in our previous studies.[31,32]

The crystal structures of the $0.5PbTiO_3-0.5BiCo_{1-x}Fe_xO_3$ ($0 \leq x \leq 1$) compounds at room temperatures were determined by using a lab X-ray diffractometer (XRD, D8 ADVANCE, Bruker). The temperature dependence of the synchrotron X-ray diffraction (SXRD) experiment was performed at the 11-ID-C beamline with an Advanced Photon Source ($\lambda = 0.117418$ Å). Detailed structural analysis was performed by the Rietveld method using the FullProf software with the same initial space group (SG) of pristine PT (SG: $P4mm$).[28]

The first-principles calculations of $0.5PbTiO_3-0.5BiCo_{1-x}Fe_xO_3$ ($x = 0, 0.5$, and 1) were conducted with CASTEP to obtain the electronic density information.[33] The PBE functions in the generalized density approximation (GGA) form were used to simulate the exchange-correlation items in the Hamiltonian.[34,35] An optimized norm-conserving psedopotential in the Kleinman−Bylander form was applied; thus, a small plane basis was set without compromising the accuracy needed for the calculations.[36,37] The kinetic energy cutoff was set to be 800 eV, and the Monkhorst−Pack k-point mesh spanning was less than 0.03 Å^{-1} in the Brillouin calculations.[38] In addition, to deal with the Pb/Bi and Ti/Co/Fe disorder during the calculations, the virtual crystal approximation (VCA) algorithm was applied.[39]

■ RESULTS AND DISCUSSION

The laboratory XRD patterns of the $0.5PbTiO_3-0.5BiCo_{1-x}Fe_xO_3$ ($0 \leq x \leq 1$) compounds at room temperature (RT) are shown in Figure 1a. The powder samples were of high quality with negligible impurity, and all of them mainly show a single tetragonal perovskite structure. The very weak reflection around 28° for Co-rich side ($x \leq 0.2$) is unidentified
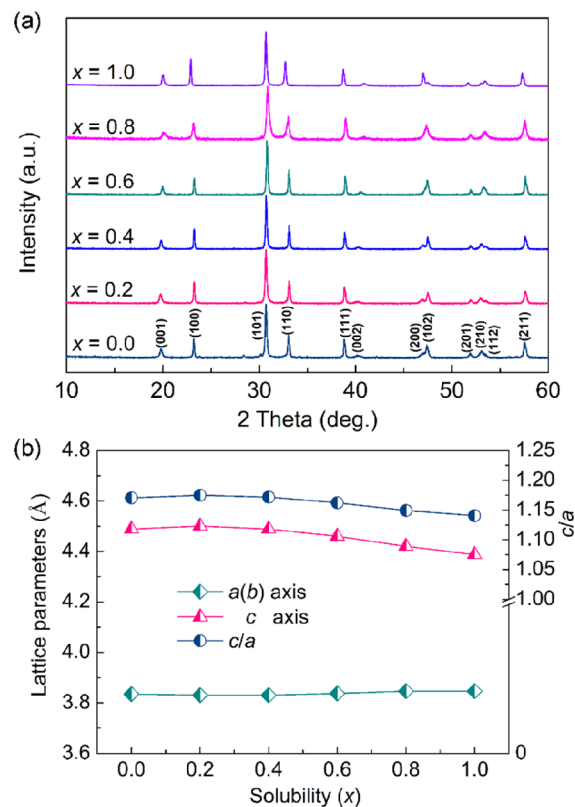

Figure 1. (a) XRD patterns and (b) lattice parameters of the $0.5PbTiO_3-0.5BiCo_{1-x}Fe_xO_3$ ($x = 0, 0.2, 0.4, 0.6, 0.8$, and 1.0) compounds at room temperature.

impurity in addition to the main tetragonal phase, which is usually observed in $BiCoO_3$-based derivatives.[40] The precise lattice parameters of the $0.5PbTiO_3-0.5BiCo_{1-x}Fe_xO_3$ ($0 \leq x \leq 1$) compounds were determined from the Rietveld refined results of the SXRD data (see the Supporting Information Figures S1–S6). Our previous report suggested that pristine $0.5PbTiO_3-0.5BiCoO_3$ had large tetragonality, with a c/a ratio of 1.17. Notably, the separation between (001) and (100) peaks decreased slightly with substitution of moderately ferroelectric-active Fe^{3+} for strongly ferroelectric-active Co^{3+}, which suggested a decrease in the c/a ratio. Detailed structural parameters are shown in Figure 1b. As can be seen, the c-axis of $0.5PbTiO_3-0.5BiCo_{1-x}Fe_xO_3$ showed a slight decrease with the replacement of Fe for Co, while the $a(b)$-axes showed the opposite trend. Consequently, the c/a ratio decreased slightly as a function of Fe content. The c/a ratio decreased from 1.17 for pristine $0.5PbTiO_3-0.5BiCoO_3$ ($x = 0$), to 1.16 for $0.5PbTiO_3-0.5BiCo_{0.4}Fe_{0.6}O_3$ ($x = 0.6$), and finally to 1.14 of $0.5PbTiO_3-0.5BiFeO_3$ ($x = 1$). The reduced tetragonality in the $0.5PbTiO_3-0.5BiCo_{1-x}Fe_xO_3$ was related to the suppressed P_S because the hybridization between the A/B-site cations and oxygens was weakened.

In perovskite-type ferroelectrics, P_S will originate from the displacements of the A/B-site atoms relative to the centroid oxygen polyhedrons (see the inset of Figure 2a).[27] Notably, the P_S displacements of the A-site Pb/Bi (δz_A) and B-site Ti/Co/ Fe (δz_B) atoms could be extracted from the structural data of the Rietveld refined results of the SXRD data. Related P_S can be estimated via the following formula[41] by simply assuming a purely ionic crystal and neglecting the electronic polarization:

$$P_S = Z \sum_i \frac{\delta z_i q_i}{V} \tag{1}$$

where δz_i indicates the cation displacement toward the ferroelectric axis of the ith ion with an electric charge of q_i, V is the unit cell volume, and Z is 1. According to the results, both δz_A and δz_B show similar decrease tendency as a function of Fe content (Figure 2a). As a result, the P_S also showed a decrease through the substitution of Fe, where the value of P_S was as high as $\sim$98 $\mu C/cm^2$ for pristine $0.5PbTiO_3-$ $0.5BiCoO_3$, $\sim$94 $\mu C/cm^2$ for $0.5PbTiO_3-0.5BiCo_{0.4}Fe_{0.6}O_3$, and finally decreased to 83 $\mu C/cm^2$ for $0.5PbTiO_3-0.5BiFeO_3$ (Figure 2b), in which strongly ferroelectric-active Co^{3+} was fully replaced by moderately ferroelectric-active Fe^{3+}.

In PT-based NTE materials, the variation of P_S will be closely related to the ferroelectric volume effect and, consequently, the NTE property.[3,26] Accordingly, the thermal expansion properties of the $0.5PbTiO_3-0.5BiCo_{1-x}Fe_xO_3$ ($x = 0, 0.2, 0.4, 0.6, 0.8,$ and 1.0) compounds were systematically studied (Figure 3). For pristine $0.5PbTiO_3-0.5BiCoO_3$ ($x = 0$), it first exhibited slightly positive thermal expansion in the ferroelectric phase. However, upon approaching the T_C, a large volume contraction of -4.8% occurred during the FE-to-PE phase transition (Figure 3a), which has never observed in PT-based NTE materials. With the substitution of Fe for Co, the volume contraction gradually decreased. Volume shrinkage during the FE-to-PE phase transition reduced from -4.8% for pristine $0.5PbTiO_3-0.5BiCoO_3$ to -4.5%, -4.2%, and -3.3% for $0.5PbTiO_3-0.5BiCo_{0.8}Fe_{0.2}O_3$ ($x = 0.2$), $0.5PbTiO_3-$ $0.5BiCo_{0.6}Fe_{0.4}O_3$ ($x = 0.4$), and $0.5PbTiO_3-0.5BiCo_{0.4}Fe_{0.6}O_3$ ($x = 0.6$) (Figures 3b–d), respectively. With further increasing Fe content, such as $x > 0.6$, it was intriguing to observe that the thermal expansion transformed from large volume contraction in a narrow temperature range to a nonlinear strong NTE in a wide temperature range. For example, for the $0.5PbTiO_3-$ $0.5BiCo_{0.2}Fe_{0.8}O_3$ compound, in the temperature range of RT to 400 °C, the unit cell volume shows little dependence on the temperature with an average CTE of $-2.26 \times 10^{-6}/°C$ (see the dashed black box in Figure 3e). However, a very strong NTE occurs on approaching the T_C. The average volumetric CTE in the whole temperature range of RT to 600 °C was $-6.12 \times 10^{-5}/°C$. Similar phenomenon was also observed in the $0.5PbTiO_3-0.5BiFeO_3$ ($x = 1.0$) compound. In the temperature of RT to 300 °C, a low CTE of $-7.2 \times 10^{-6}/°C$ was observed (see the dashed black box in Figure 3f), while a sharply decrease of unit cell volume occurs with further increasing temperature. The overall CTE of $0.5PbTiO_3-$ $0.5BiFeO_3$ is $-4.15 \times 10^{-5}/°C$ in the temperature range of RT to 640 °C. Notably, the present nonlinear NTE was even stronger than many representative large NTE compounds, such as $Cd(CN)_2$ ($\bar{\alpha}_V = -3.4 \times 10^{-5}/°C$, -103 to -102 °C),[42] $LaFe_{10.5}Co_{1.0}Si_{1.5}$ ($\bar{\alpha}_V = -2.6 \times 10^{-5}/°C$, -33 to 77 °C),[43] $SrCu_3Fe_4O_{12}$ ($\bar{\alpha}_V = -2.0 \times 10^{-5}/°C$, -93 to -23 °C),[44] and $Fe[Co(CN)_6]$ ($\bar{\alpha}_V = -4.41 \times 10^{-6}/°C$, -268.8 to 27 °C).[45] NTE Materials with large magnitude of NTE and wide NTE operation temperature windows are preferable for practical applications, as they can be used to tailor the CTE
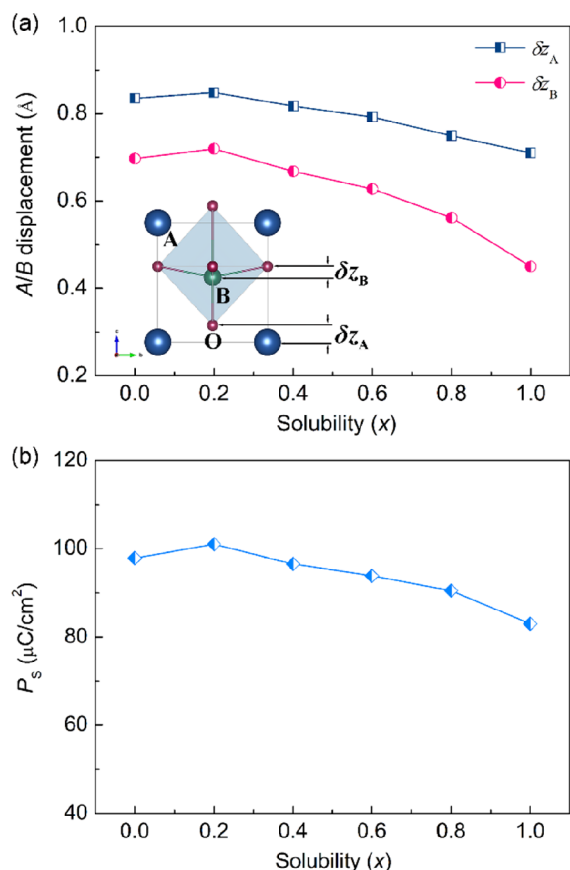

Figure 2. Calculated displacements of the A-site (δ_A) and B-site (δ_B) cations (a) and (b) spontaneous polarization (P_S) of the $0.5PbTiO_3-$ $0.5BiCo_{1-x}Fe_xO_3$ ($x = 0, 0.2, 0.4, 0.6, 0.8,$ and 1.0) compounds at room temperature. The inset shows a schematic diagram of the P_S displacements.
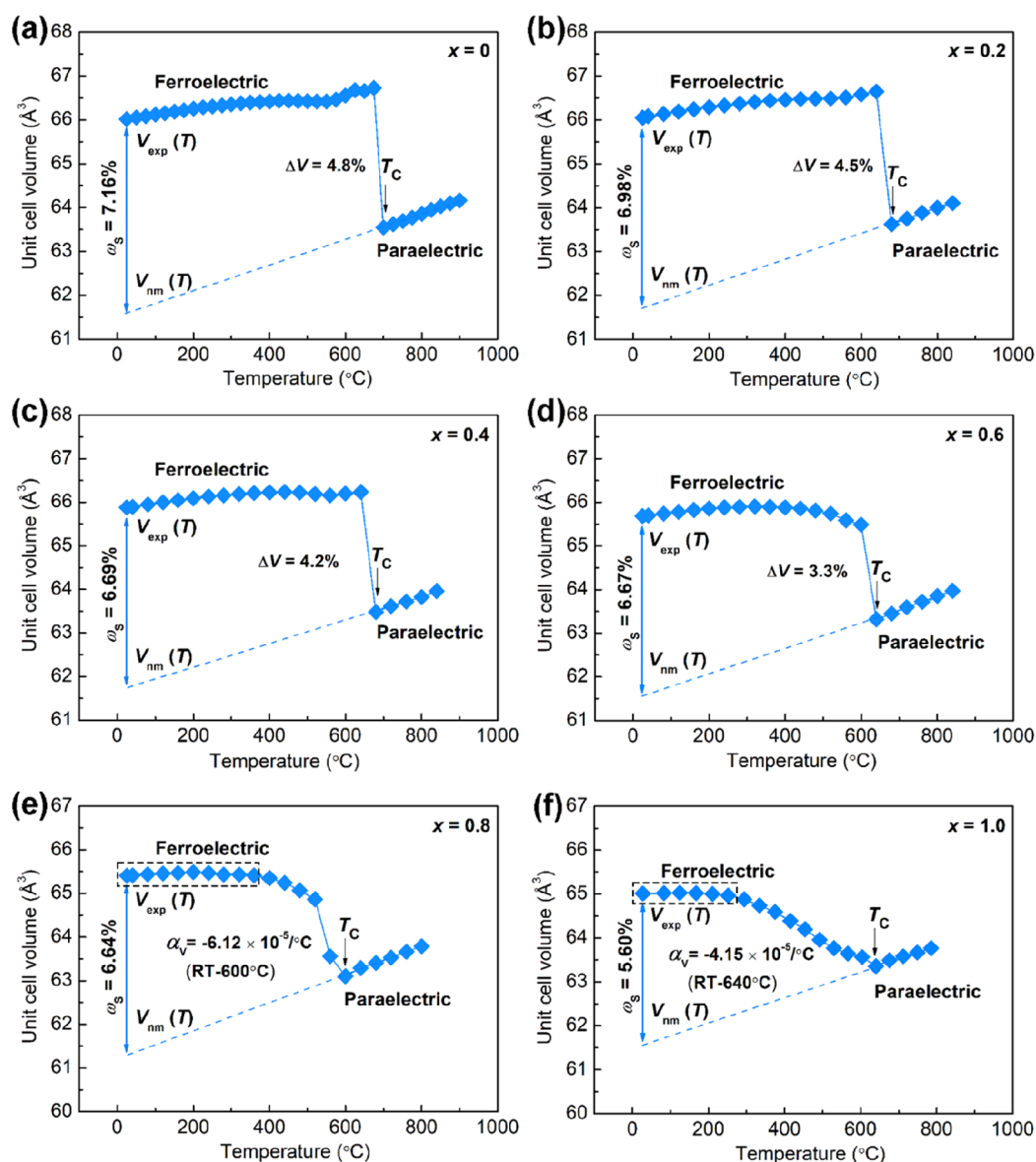
Figure 3. Temperature dependence of the unit cell volume of the $0.5PbTiO_3-0.5BiCo_{1-x}Fe_xO_3$ compounds: (a) $x = 0$, (b) $x = 0.2$, (c) $x = 0.4$, (d) $x = 0.6$, (e) $x = 0.8$, and (f) $x = 1.0$.

of materials more efficiently, compared to NTE materials that can only operate in a limited temperature range.

Both the first-principles calculations and the lattice dynamics theory suggested that the evolution of ferroelectric properties was closely related to the NTE of the PT-based ferroelectrics.[3] Recently, a proposed new physical concept of spontaneous volume ferroelectrostriction (SVFS) can be used to explain the origin of NTE in the PT-based ferroelectrics.[9] The SVFS (ω_S) can be used to quantitatively interpret the effect of ferroelectricity that will contribute to the unusual changes in the unit cell volume of the tetragonal ferroelectric phase. Generally, a large ω_S value will indicate a strong NTE and a large volume contribution by ferroelectricity, while a smaller value will indicate a weak NTE. SVFS can be defined by

$$\omega_S = \frac{V_{exp} - V_{nm}}{V_{nm}} \times 100\% \tag{2}$$

In the equation V_{exp} and V_{nm} indicate unit cell volumes of the experimental and nominal ones, respectively, and V_{nm} can be

obtained by extrapolation from the PE to FE phase. In this work, the ω_S values were 7.16%, 6.98%, 6.69%, 6.67%, 6.64%, and 5.60% for $0.5PbTiO_3-0.5BiCoO_3$ ($x = 0$), $0.5PbTiO_3-0.5BiCo_{0.8}Fe_{0.2}O_3$ ($x = 0.2$), $0.5PbTiO_3-0.5BiCo_{0.6}Fe_{0.4}O_3$ ($x = 0.4$), $0.5PbTiO_3-0.5BiCo_{0.4}Fe_{0.6}O_3$ ($x = 0.6$), $0.5PbTiO_3-0.5BiCo_{0.2}Fe_{0.8}O_3$ ($x = 0.8$), and $0.5PbTiO_3-0.5BiFeO_3$ ($x = 1.0$), respectively, which were consistent with the gradually weakened NTE during the FE-to-PE phase transition.

In the ABO_3 perovskite-type ferroelectrics, the hybridizations between the A/B-site cations and oxygens were important for lattice distortion and ferroelectricity.[46−50] To take a deep insight into the effects of Fe substitution on ferroelectricity and NTE behavior, we performed first-principles calculations of the electronic density distribution for $0.5PbTiO_3-0.5BiCo_{1-x}Fe_xO_3$ ($x = 0$, 0.5, and 1.0) (Figure 4). In pristine $0.5PbTiO_3-0.5BiCoO_3$ without Fe substitution, during bond formation, electron transformation from Co/Ti to the oxygens was observed, and the electronic cloud around the Co/Ti−O bonds showed a remarkable spatial orientation
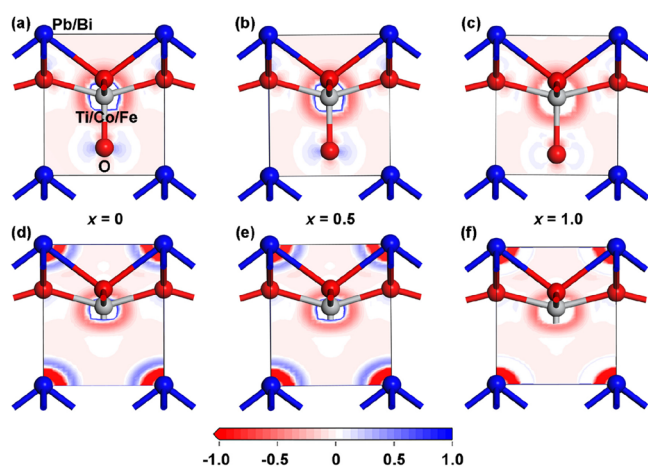
Figure 4. Electron density difference map around the Ti/Co/Fe—O bonds in (a) $0.5PbTiO_3-0.5BiCoO_3$, (b) $0.5PbTiO_3-0.5Bi-Co_{0.5}Fe_{0.5}O_3$, and (c) $0.5PbTiO_3-0.5BiFeO_3$ and Pb/Bi—O bonds in (d) $0.5PbTiO_3-0.5BiCoO_3$, (e) $0.5PbTiO_3-0.5BiCo_{0.5}Fe_{0.5}O_3$, and (f) $0.5PbTiO_3-0.5BiFeO_3$. The Pb/Bi, Ti/Co/Fe, and O atoms are displayed by blue, gray, and red balls, respectively.

(Figure 4a), suggesting strong orbital hybridization, resulting in large lattice distortions. With the substitution of moderately ferroelectric-active Fe for strongly ferroelectric-active Co, such as $0.5PbTiO_3-0.5BiCo_{0.5}Fe_{0.5}O_3$, the anisotropic properties of the electronic cloud redistribution becomes smaller than the pristine $0.5PbTiO_3-0.5BiCoO_3$ (Figure 4b). With further increases in the substitution content of Fe, the electronic cloud in the corresponding area further significantly decreased (Figure 4c). The above results suggested that orbital hybridization was weakened by Co/Fe substitution. In addition, in pristine $0.5PbTiO_3-0.5BiCoO_3$, a large electron-gaining area gathered around the Pb/Bi—O bonds, which indicates the strong covalent bonds (Figure 4d). Nevertheless, with the substitution of Fe, the electron density around the Pb/Bi—O bonds was decreased (Figure 4e). Specifically, the electron-gaining area sharply decreased in the $0.5PbTiO_3-0.5BiFeO_3$ compound, in which Co was fully replaced by Fe (Figure 4f), compared to pristine $0.5PbTiO_3-0.5BiCoO_3$, which implied that the hybridization between the Pb/Bi and O atoms was also reduced by Co/Fe substitution. Therefore, we concluded that the decrease in ferroelectricity from pristine $0.5PbTiO_3-0.5BiCoO_3$ to $0.5PbTiO_3-0.5BiFeO_3$ resulted from the decreased orbital hybridization because of the Co/Fe substitution, which was consistent with the decreased P_S and c/a of the experimental results.

Materials with large NTE over a wide temperature range are preferrable in thermal-expansion-control engineering.[1−3] The work presented a method for transforming phase-transition-type NTE materials to nonlinear strong NTE in a wide temperature window in PT-based ferroelectrics. Inspired by this study, other polar perovskites with large volume contraction during the FE-to-PE phase transition, such as $PbTi_{1-x}V_xO_3$,[31] could also realize nonlinear strong NTE in an extended temperature range by replacing the strongly ferro-electric-active atoms (such as Pb, Bi, Ti, and V) with weakly ferroelectric-active atoms, such as Sr, La, Mg, In, and Zr.[30] In addition, this type of material design by controlling the degree of lattice distortion could also be applied in other lead-free tetragonal compounds $BiCoO_3$ and $Bi(Zn_{1/2}Ti_{1/2})O_3$,[40,51] as these perovskite compounds with giant tetragonalities are

treated as potential matrices for lead-free ferroelectric/piezoelectric materials.

CONCLUSIONS

In conclusion, the NTE behavior of $0.5PbTiO_3-0.5BiCoO_3$ tetragonal compound was well controlled from a large volume contraction in a limited range to nonlinear strong NTE over a wide temperature range. The detailed crystal structure and chemical bonds were systematically studied by synchrotron X-ray diffraction and DFT calculations. The controllable NTE was closely related to the tunable spontaneous volume ferroelectrostriction by modifying the cation ratio with different ferroelectric activity, i.e., strongly ferroelectric-active Co replaced by moderately ferroelectric-active Fe. The present study enriched the NTE family and also provided a simple but effective method to tailor the thermal expansion properties of ferroelectric NTE materials.

ASSOCIATED CONTENT

Supporting Information

The Supporting Information is available free of charge at https://pubs.acs.org/doi/10.1021/acsami.2c00771.

Details of Rietveld refinement of SXRD patterns of $0.5PbTiO_3-0.5BiCo_{1-x}Fe_xO_3$ (x = 0, 0.2, 0.4, 0.6, 0.8, and 1.0) (PDF)

AUTHOR INFORMATION

Corresponding Authors

Zhao Pan — Beijing National Laboratory for Condensed Matter Physics, Institute of Physics, Chinese Academy of Sciences, Beijing 100190, China; orcid.org/0000-0002-8693-2508; Email: zhaopan@iphy.ac.cn

Jun Chen — Beijing Advanced Innovation Center for Materials Genome Engineering and Department of Physical Chemistry, University of Science and Technology Beijing, Beijing 100083, China; orcid.org/0000-0002-7330-8976; Email: junchen@ustb.edu.cn

Authors

Xingxing Jiang — Center for Crystal R&D, Key Laboratory of Functional Crystals and Laser Technology, Technical Institute of Physics and Chemistry, Chinese Academy of Sciences, Beijing 100190, China; orcid.org/0000-0001-6068-8773

Runze Yu — Beijing National Laboratory for Condensed Matter Physics, Institute of Physics, Chinese Academy of Sciences, Beijing 100190, China; orcid.org/0000-0001-9889-0299

Yang Ren — X-ray Science Division, Argonne National Laboratory, Argonne, Illinois 60439, United States; orcid.org/0000-0001-9831-6035

Zheshuai Lin — Center for Crystal R&D, Key Laboratory of Functional Crystals and Laser Technology, Technical Institute of Physics and Chemistry, Chinese Academy of Sciences, Beijing 100190, China; orcid.org/0000-0002-9829-9893

Masaki Azuma — Laboratory for Materials and Structures, Tokyo Institute of Technology, Yokohama 226-8503, Japan; orcid.org/0000-0002-8378-321X

Xianran Xing — Beijing Advanced Innovation Center for Materials Genome Engineering and Department of Physical

Chemistry, University of Science and Technology Beijing, Beijing 100083, China; ● orcid.org/0000-0003-0704-8886

Complete contact information is available at:
https://pubs.acs.org/10.1021/acsami.2c00771

Author Contributions

Notes

■ ACKNOWLEDGMENTS

■ REFERENCES

(1) Evans, J. S. O. Negative Thermal Materials. *J. Chem. Soc. Dalton. Trans.* **1999**, *19*, 3317−3326.

(2) Takenaka, K. Negative Thermal Expansion Materials: Technological Key for Control of Thermal Expansion. *Sci. Technol. Adv. Mater.* **2012**, *13*, 013001.

(3) Chen, J.; Hu, L.; Deng, J.; Xing, X. Negative Thermal Expansion in Functional Materials: Controllable Thermal Expansion by Chemical Modifications. *Chem. Soc. Rev.* **2015**, *44*, 3522−3567.

(4) Liu, H.; Sun, W.; Zhang, Z.; Lovings, L. N.; Lind, C. Thermal Expansion Behavior in the $A_2M_3O_{12}$ Family of Materials. *Solids* **2021**, *2*, 87−107.

(5) Yang, X.; Xu, J.; Li, H.; Cheng, X.; Yan, X. In Situ Synthesis of ZrO_2/ZrW_2O_8 Composites with Near-Zero Thermal Expansion. *J. Am. Ceram. Soc.* **2007**, *90*, 1953−1955.

(6) Ding, L.; Wang, C.; Na, Y.; Chu, L.; Yan, J. Preparation and Near Zero Thermal Expansion Property of $Mn_3Cu_{0.5}A_{0.5}N$ (A = Ni, Sn)/Cu Composites. *Scripta. Mater.* **2011**, *65*, 687−690.

(7) Qiao, Y.; Xiao, N.; Song, Y.; Deng, S.; Huang, R.; Li, L.; Xing, X.; Chen, J. Achieving High Performances of Ultra-Low Thermal Expansion and High Thermal Conductivity in $0.5PbTiO_3$-0.5-$(Bi_{0.9}La_{0.1})FeO_3$@Cu Core-Shell Composite. *ACS Appl. Mater. Interfaces* **2020**, *12*, 57228−57234.

(8) Song, X.; Sun, Z.; Huang, Q.; Rettenmayr, M.; Liu, X.; Seyring, M.; Li, G.; Rao, G.; Yin, F. Adjustable Zero Thermal Expansion in Antiperovskite Manganese Nitride. *Adv. Mater.* **2011**, *23*, 4690−4694.

(9) Chen, J.; Wang, F.; Huang, Q.; Hu, L.; Song, X.; Deng, J.; Yu, R.; Xing, X. Effectively Control Negative Thermal Expansion of Single-phase Ferroelectrics of $PbTiO_3$-$(Bi,La)FeO_3$ over a Giant Range. *Sci. Rep.* **2013**, *3*, 2458.

(10) Nakajima, N.; Yamamura, Y.; Tsuji, T. Synthesis and Physical Properties of Negative Thermal Expansion Materials $Zr_{1-x}M_xW2O_{8-y}$ (M = Sc, In, Y) Substituted for Zr(IV) Sites by M(III) Ions. *Solid State Commun.* **2003**, *128*, 193−196.

(11) Chapman, K. W.; Chupas, P. J.; Kepert, C. J. Compositional Dependence of Negative Thermal Expansion in the Prussian Blue Analogues $M^{II}Pt^{IV}(CN)_6$ (M = Mn, Fe, Co, Ni, Cu, Zn, Cd). *J. Am. Chem. Soc.* **2006**, *128*, 7009−7014.

(12) Oka, K.; Nabetani, K.; Sakaguchi, C.; Seki, H.; Czapski, M.; Shimakawa, Y.; Azuma, M. Tuning Negative Thermal Expansion in $Bi_{1-x}Ln_xNiO_3$ (*Ln* = La, Nd, Eu, Dy). *Appl. Phys. Lett.* **2013**, *103*, 061909.

(13) Asai, D.; Mizuno, Y.; Hasegawa, H.; Yokoyama, Y.; Okamoto, Y.; Katayama, N.; Suzuki, H. S.; Imanaka, Y.; Takenaka, K. Valence Fluctuations and Giant Isotropic Negative Thermal Expansion in $Sm_{1-x}R_xS$ (R = Y, La, Ce, Pr, Nd). *Appl. Phys. Lett.* **2019**, *114*, 141902.

(14) Suzuki, T.; Omote, A. Zero Thermal Expansion in $(Al_{2x}(HfMg)_{1-x})(WO_4)_3$. *J. Am. Ceram. Soc.* **2006**, *89*, 691−693.

(15) Gao, Q.; Shi, N.; Sanson, A.; Sun, Y.; Milazzo, R.; Olivi, L.; Zhu, H.; Lapidus, S. H.; Zheng, L.; Chen, J.; Xing, X. Tunable Thermal Expansion from Negative, Zero, to Positive in Cubic Prussian Blue Analogues of $GaFe(CN)_6$. *Inorg. Chem.* **2018**, *57*, 14027−14030.

(16) Sun, W.; Zhang, H.; Li, W.; Huang, R.; Zhao, Y.; Wang, W.; Li, L. Controllable Negative Thermal Expansion in $NaZn_{13}$-type La(Fe, Co, Al)$_{13}$ Compounds. *AIP Adv.* **2020**, *10*, 075123.

(17) Yang, C.; Zhang, Y.; Bai, J.; Tong, P.; Lin, J.; Tong, H.; Zhang, L.; Wen, W.; Zhang, X.; Sun, Y. Isotropic Low Thermal Expansion over a Wide Temperature Range in $Ti_{1-x}Zr_xF_{3+x}$ ($0.1 \leq x \leq 0.5$) Solid Solutions. *Inorg. Chem.* **2018**, *57*, 14396−14400.

(18) Liu, Y.; Mei, D.; Wang, N.; Molokeev, M. S.; Jiang, X.; Lin, Z. Intrinsic Isotropic Near-Zero Thermal Expansion in $Zn_4B_6O_{12}X$ (X = O, S, Se). *ACS Appl. Mater. Interfaces* **2020**, *12*, 38435−38440.

(19) Takenaka, K.; Asai, D.; Kaizu, R.; Mizuno, Y.; Yokoyama, Y.; Okamoto, Y.; Katayama, N.; Suzuki, H. S.; Imanaka, Y. Giant Isotropic Negative Thermal Expansion in Y-Doped Samarium Monosulfides by Intra-Atomic Charge Transfer. *Sci. Rep.* **2019**, *9*, 122.

(20) Xing, X.; Deng, J.; Chen, J.; Liu, G. Novel Thermal Expansion of Lead Titanate. *Rare Metals* **2003**, *22*, 294−297.

(21) Chen, J.; Xing, X.; Yu, R.; Liu, G. Thermal Expansion Properties of Lanthanum-Substituted Lead Titanate Ceramics. *J. Am. Ceram. Soc.* **2005**, *88*, 1356−1358.

(22) Yamamoto, H.; Imai, T.; Sakai, Y.; Azuma, M. Colossal Negative Thermal Expansion in Electron-Doped $PbVO_3$. *Angew. Chem., Int. Ed.* **2018**, *57*, 8170−8173.

(23) Pan, Z.; Jiang, X.; Nishikubo, T.; Sakai, Y.; Ishizaki, H.; Oka, K.; Lin, Z.; Azuma, M. Pronounced Negative Thermal Expansion in Lead-Free $BiCoO_3$-Based Ferroelectrics Triggered by the Stabilized Perovskite Structure. *Chem. Mater.* **2019**, *31*, 6187−6192.

(24) Chen, J.; Xing, X.; Yu, R.; Liu, G. Structure and Enhancement of Negative Thermal Expansion in the $PbTiO_3$-$CdTiO_3$ System. *Appl. Phys. Lett.* **2005**, *87*, 231915.

(25) Chen, J.; Xing, X.; Liu, G.; Li, J.; Liu, Y. Structure and Negative Thermal Expansion in the $PbTiO_3$-$BiFeO_3$ System. *Appl. Phys. Lett.* **2006**, *89*, 101914.

(26) Pan, Z.; Chen, J.; Yu, R.; Patra, L.; Ravindran, P.; Sanson, A.; Milazzo, R.; Carnera, A.; Hu, L.; Wang, L.; Yamamoto, H.; Ren, Y.; Huang, Q.; Sakai, Y.; Nishikubo, T.; Ogata, T.; Fan, X.; Li, Y.; Li, G.; Hojo, H.; Azuma, M.; Xing, X. Large Negative Thermal Expansion Induced by Synergistic Effects of Ferroelectrostriction and Spin Crossover in $PbTiO_3$-Based Perovskites. *Chem. Mater.* **2019**, *31*, 1296−1303.

(27) Chen, J.; Xing, X.; Sun, C.; Hu, P.; Yu, R.; Wang, X.; Li, L. Zero Thermal Expansion in $PbTiO_3$-Based Perovskites. *J. Am. Chem. Soc.* **2008**, *130*, 1144−1145.

(28) Chen, J.; Nittala, K.; Forrester, J. S.; Jones, J. L.; Deng, J.; Yu, R.; Xing, X. The Role of Spontaneous Polarization in the Negative Thermal Expansion of Tetragonal $PbTiO_3$-Based Compounds. *J. Am. Chem. Soc.* **2011**, *133*, 11114−11117.

(29) Grinberg, I.; Suchomel, M. R.; Davies, P. K.; Rappe, A. M. Predicting Morphotropic Phase Boundary Locations and Transition Temperatures in Pb- and Bi-Based Perovskite Solid Solutions from Crystal Chemical Data and First-Principles Calculations. *J. Appl. Phys.* **2005**, *98*, 094111.

(30) Grinberg, I.; Rappe, A. M. First Principles Calculations, Crystal Chemistry and Properties of Ferroelectric Perovskites. *Phase Transit.* **2007**, *80*, 351−368.

(31) Pan, Z.; Chen, J.; Jiang, X.; Hu, L.; Yu, R.; Yamamoto, H.; Ogata, T.; Hattori, Y.; Guo, F.; Fan, X.; Li, Y.; Li, G.; Gu, H.; Ren, Y.; Lin, Z.; Azuma, M.; Xing, X. Colossal Volume Contraction in Strong Polar Perovskites of Pb(Ti, V)O$_3$. *J. Am. Chem. Soc.* **2017**, *139*, 14865−14868.

(32) Pan, Z.; Zhang, M.; Nishikubo, T.; Sakai, Y.; Yamamoto, H.; Hojo, H.; Fukuda, M.; Hu, L.; Ishizaki, H.; Kaneko, S.; Kawaguchi, S.; Koruza, J.; Rödel, J.; Azuma, M. Polarization Rotation at Morphotropic Phase Boundary in New Lead-Free Na$_{1/2}$Bi$_{1/2}$V$_{1-x}$Ti$_x$O$_3$ Piezoceramics. *ACS Appl. Mater. Interfaces* **2021**, *13*, 5208−5215.

(33) Kohn, W.; Sham, L. J. Self-Consistent Equations Including Exchange and Correlation Effects. *Phys. Rev.* **1965**, *140*, A1133−A1138.

(34) Perdew, J. P.; Burke, K.; Ernzerhof, M. Generalized Gradient Approximation Made Simple. *Phys. Rev. Lett.* **1996**, *77*, 3865−3868.

(35) Perdew, J. P.; Wang, Y. Pair-Distribution Function and Its Coupling-Constant Average for the Spin-Polarized Electron Gas. *Phys. Rev. B: Condens Matter Mater. Phys.* **1992**, *46*, 12947−12954.

(36) Hamann, D. R.; Schlüter, M.; Chiang, C. Norm-Conserving Pseudopotentials. *Phys. Rev. Lett.* **1979**, *43*, 1494−1497.

(37) Kleinman, L.; Bylander, D. M. Efficacious Form for Model Pseudopotentials. *Phys. Rev. Lett.* **1982**, *48*, 1425−1428.

(38) Monkhorst, H. J.; Pack, J. D. Special Points for Brillouin-Zone Integrations. *Phys. Rev. B: Solid State* **1976**, *13*, 5188−5192.

(39) Bellaiche, L.; Vanderbilt, D. Virtual Crystal Approximation Revisited: Application to Dielectric and Piezoelectric Properties of Perovskites. *Phys. Rev. B: Condens Matter Mater. Phys.* **2000**, *61*, 7877−7882.

(40) Belik, A. A.; Iikubo, S.; Kodama, K.; Igawa, N.; Shamoto, S.; Niitaka, S.; Azuma, M.; Shimakawa, Y.; Takano, M.; Izumi, F.; Takayama-Muromachi, E. Neutron Powder Diffraction Study on the Crystal and Magnetic Structures of BiCoO$_3$. *Chem. Mater.* **2006**, *18*, 798−803.

(41) Frantti, J.; Ivanov, S.; Eriksson, S.; Rundlöf, H.; Lantto, V.; Lappalainen, J.; Kakihana, M. Phase Transitions of Pb(Zr$_x$Ti$_{1-x}$)O$_3$ Ceramics. *Phys. Rev. B: Condens. Matter Mater. Phys.* **2002**, *66*, 064108.

(42) Phillips, A. E.; Goodwin, A. L.; Halder, G. J.; Southon, P. D.; Kepert, C. J. Nanoporosity and Exceptional Negative Thermal Expansion in Single-Network Cadmium Cyanide. *Angew. Chem., Int. Ed.* **2008**, *47*, 1396−1399.

(43) Huang, R. J.; Liu, Y.; Fan, W.; Tan, J.; Xiao, F.; Qian, L.; Li, L. Giant Negative Thermal Expansion in NaZn$_{13}$-type La(Fe, Si, Co)$_{13}$ Compounds. *J. Am. Chem. Soc.* **2013**, *135*, 11469−11472.

(44) Yamada, I.; Tsuchida, K.; Ohgushi, K.; Hayashi, N.; Kim, J.; Tsuji, N.; Takahashi, R.; Matsushita, M.; Nishiyama, N.; Inoue, T.; Irifune, T.; Kato, K.; Takata, M.; Takano, M. Giant Negative Thermal Expansion in the Iron Perovskite SrCu$_3$Fe$_4$O$_{12}$. *Angew. Chem., Int. Ed.* **2011**, *50*, 6579−6582.

(45) Margadonna, S.; Prassides, K.; Fitch, A. N. Zero Thermal Expansion in a Prussian Blue Analogue. *J. Am. Chem. Soc.* **2004**, *126*, 15390−15391.

(46) Kuroiwa, Y.; Aoyagi, S.; Sawada, A.; Harada, J.; Nishibori, E.; Takata, M.; Sakata, M. Evidence for Pb-O Covalency in Tetragonal PbTiO$_3$. *Phys. Rev. Lett.* **2001**, *87*, 217601.

(47) Yashima, M.; Omoto, K.; Chen, J.; Kato, H.; Xing, X. Evidence for (Bi,Pb)-O Covalency in the High T_C Ferroelectric PbTiO$_3$-BiFeO$_3$ with Large Tetragonality. *Chem. Mater.* **2011**, *23*, 3135−3137.

(48) Pan, Z.; Chen, J.; Yu, R.; Yamamoto, H.; Rong, Y.; Hu, L.; Li, Q.; Lin, K.; You, L.; Zhao, K.; Fan, L.; Ren, Y.; Kato, K.; Azuma, M.; Xing, X. Giant Polarization and High Temperature Monoclinic Phase in a Lead-Free Perovskite of Bi(Zn$_{0.5}$Ti$_{0.5}$)O$_3$-BiFeO$_3$. *Inorg. Chem.* **2016**, *55*, 9513−9516.

(49) Fan, L.; Li, Q.; Zhang, L.; Shi, N.; Liu, H.; Ren, Y.; Chen, J.; Xing, X. Negative Thermal Expansion and the Role of Hybridization

in Perovskite-type PbTiO$_3$-Bi(Cu$_{0.5}$Ti$_{0.5}$)O$_3$. *Inorg. Chem. Front.* **2020**, *7*, 1190−1195.

(50) Pan, Z.; Fang, Y.; Nishikubo, T.; Hu, L.; Kawaguchi, S.; Azuma, M. Tolerance Factor Control of Tetrgonality and Negative Thermal Expansion in PbTiO$_3$-Based Ferroelectrics. *Chem. Mater.* **2022**, *34*, 2798−2803.

(51) Suchomel, M. R.; Fogg, A. M.; Allix, M.; Niu, H.; Claridge, J. B.; Rosseinsky, M. J. Bi$_2$ZnTiO$_6$: A Lead-Free Closed-Shell Polar Perovskite with a Calculated Ionic Polarization of 150 μC cm^{-2}. *Chem. Mater.* **2006**, *18*, 4987−4989.